NASA/TM—2004-213420 AIAA–2004–1638

Implementation of Improved Transverse Shear Calculations and Higher Order Laminate Theory Into Strain Rate Dependent Analyses of Polymer Matrix Composites

Linfa Zhu, Heung Soo Kim, and Aditi Chattopadhyay
Arizona State University, Tempe, Arizona

Robert K. Goldberg
Glenn Research Center, Cleveland, Ohio

December 2004

The NASA STI Program Office . . . in Profile

Since its founding, NASA has been dedicated to the advancement of aeronautics and space science. The NASA Scientific and Technical Information (STI) Program Office plays a key part in helping NASA maintain this important role.

The NASA STI Program Office is operated by Langley Research Center, the Lead Center for NASA's scientific and technical information. The NASA STI Program Office provides access to the NASA STI Database, the largest collection of aeronautical and space science STI in the world. The Program Office is also NASA's institutional mechanism for disseminating the results of its research and development activities. These results are published by NASA in the NASA STI Report Series, which includes the following report types:

- TECHNICAL PUBLICATION. Reports of completed research or a major significant phase of research that present the results of NASA programs and include extensive data or theoretical analysis. Includes compilations of significant scientific and technical data and information deemed to be of continuing reference value. NASA's counterpart of peer-reviewed formal professional papers but has less stringent limitations on manuscript length and extent of graphic presentations.

- TECHNICAL MEMORANDUM. Scientific and technical findings that are preliminary or of specialized interest, e.g., quick release reports, working papers, and bibliographies that contain minimal annotation. Does not contain extensive analysis.

- CONTRACTOR REPORT. Scientific and technical findings by NASA-sponsored contractors and grantees.

- CONFERENCE PUBLICATION. Collected papers from scientific and technical conferences, symposia, seminars, or other meetings sponsored or cosponsored by NASA.

- SPECIAL PUBLICATION. Scientific, technical, or historical information from NASA programs, projects, and missions, often concerned with subjects having substantial public interest.

- TECHNICAL TRANSLATION. English-language translations of foreign scientific and technical material pertinent to NASA's mission.

Specialized services that complement the STI Program Office's diverse offerings include creating custom thesauri, building customized databases, organizing and publishing research results . . . even providing videos.

For more information about the NASA STI Program Office, see the following:

- Access the NASA STI Program Home Page at ***http://www.sti.nasa.gov***

- E-mail your question via the Internet to help@sti.nasa.gov

- Fax your question to the NASA Access Help Desk at 301–621–0134

- Telephone the NASA Access Help Desk at 301–621–0390

- Write to:
  NASA Access Help Desk
  NASA Center for AeroSpace Information
  7121 Standard Drive
  Hanover, MD 21076

NASA/TM—2004-213420 AIAA–2004–1638

Implementation of Improved Transverse Shear Calculations and Higher Order Laminate Theory Into Strain Rate Dependent Analyses of Polymer Matrix Composites

Linfa Zhu, Heung Soo Kim, and Aditi Chattopadhyay
Arizona State University, Tempe, Arizona

Robert K. Goldberg
Glenn Research Center, Cleveland, Ohio

Prepared for the
45th Structures, Structural Dynamics, and Materials Conference
cosponsored by the AIAA, ASME, ASCE, AHS, and ASC
Palm Springs, California, April 19–22, 2004

National Aeronautics and
Space Administration

Glenn Research Center

December 2004

Acknowledgments

The authors acknowledge the support of NASA Glenn Research Center, grant number, NCC3–1024, technical monitor, Robert K. Goldberg, in conducting this research.

Available from

NASA Center for Aerospace Information
7121 Standard Drive
Hanover, MD 21076

National Technical Information Service
5285 Port Royal Road
Springfield, VA 22100

Available electronically at http://gltrs.grc.nasa.gov

Implementation of Improved Transverse Shear Calculations and Higher Order Laminate Theory into Strain Rate Dependent Analyses of Polymer Matrix Composites

Linfa Zhu, Heung Soo Kim, and Aditi Chattopadhyay
Department of Mechanical and Aerospace Engineering
Arizona State University
Tempe, Arizona 85287

Robert K. Goldberg
National Aeronautics and Space Administration
Glenn Research Center
Cleveland, Ohio 44135

Abstract

A numerical procedure has been developed to investigate the nonlinear and strain rate dependent deformation response of polymer matrix composite laminated plates under high strain rate impact loadings. A recently developed strength of materials based micromechanics model, incorporating a set of nonlinear, strain rate dependent constitutive equations for the polymer matrix, is extended to account for the transverse shear effects during impact. Four different assumptions of transverse shear deformation are investigated in order to improve the developed strain rate dependent micromechanics model. The validities of these assumptions are investigated using numerical and theoretical approaches. A method to determine through the thickness strain and transverse Poisson's ratio of the composite is developed. The revised micromechanics model is then implemented into a higher order laminated plate theory which is modified to include the effects of inelastic strains. Parametric studies are conducted to investigate the mechanical response of composite plates under high strain rate loadings. Results show the transverse shear stresses cannot be neglected in the impact problem. A significant level of strain rate dependency and material nonlinearity is found in the deformation response of representative composite specimens.

Introduction

There is a growing need in military and civil applications for composite materials that not only have good structural characteristics, but also good penetration resistance and greater strength after impact. Polymer matrix composites are very susceptible to projectile impact such as fragments, flying debris, or a failed rotor blade. If not contained, a projectile traveling at ballistic velocity could penetrate a polymer matrix composite plate or shell and cause fires, hull damage, occupant injury and component malfunction. For example, an engine containment system must be capable of containing fragments traveling at ballistic velocities from a failed fan blade. Also, such an impact event may compromise the structural integrity of the composite and lead to catastrophic failure. Thus, it is important to develop the ability to predict the deformation and failure behavior of polymer matrix composites subject to high strain rate loading conditions. An analysis methodology must be able to account for any strain rate effects, material nonlinearities, and transverse shear effects that may be present in the impact problem. Also, the computational efficiency is critical in the numerical analysis of such a problem. The objective of this work is to develop an efficient numerical framework for the analysis of engine containment systems made of polymer matrix composites addressing the issues discussed above.

Several equivalent single-layer laminate theories have been developed to investigate the mechanical response of composite laminated plates on a macroscopic scale.[1] As is well known, Classical Laminated Plate Theory (CLT) neglects the transverse shear stresses by using the Kirchhoff hypothesis. By relaxing the Kirchhoff hypothesis, i.e., by allowing the transverse normals to not necessarily remain perpendicular to the deformed midsurface of the composite laminate, the First-Order Shear Deformation Laminated Plate Theory (FSDT) was developed.[2] In FSDT, transverse shear strains are represented as constant through the laminate thickness and shear correction factors are used to model the transverse shear deformation. By assuming a cubic displacement field, a more accurate theory, Higher Order Laminated Plate Theory (HOT), was developed.[3,4] In HOT, transverse shear stresses are modeled by assuming cubic displacement fields through the laminate thickness, thereby eliminating the need for shear correction factors. Also, unlike FSDT, the conditions of zero transverse shear stresses on the top and bottom surfaces are satisfied by imposing these criteria as constraints.

Various micromechanics models have been developed to characterize the nonlinear properties of polymer matrix composites. In micromechanics, the overall properties and response of the composite are computed based on the properties and response of the individual constituents. Plasticity and viscoplasticity based constitutive equations can be used to compute the nonlinear response of the matrix constituent (assuming the fiber is linear elastic, as is usually the case for polymer matrix composites), and homogenization methods can then be applied to compute the overall (nonlinear) response of the composite. The methodology is based on defining a unit cell in the composite, for which the behavior of the unit cell can be assumed to be equivalent to the response of the entire composite ply. Several examples of this approach have been developed previously. For example, the Method of Cells (MOC) was developed by Aboudi for unidirectional fiber-reinforced composites whose constituents were elasto-viscoplastic materials.[5] Pindera and Bednarcyk reformulated the MOC using simplified uniform stress and strain assumptions, which resulted in improving the computational efficiency of the analysis procedure considerably.[6] By applying a similar approach and discretizing the composite unit cell into three subcells, a two dimensional model that described the elastic-plastic behavior of fibrous composites was developed by Sun and Chen.[7] This model then was extended to three dimensions by Robertson and Mall.[8] A more precise elastic micromechanics model was proposed by Whitney in which the unit cell was divided into an arbitrary number of rectangular, horizontal slices.[9] Mital, Murthy and Chamis[10] used a slicing approach to compute the effective elastic constants and microstresses (fiber and matrix stresses) in ceramic matrix composites. In this work, a mechanics of materials approach was used to compute the effective elastic constants and microstresses in each slice of a unit cell. Laminate theory was then applied to obtain the effective elastic constants for the unit cell. Laminate theory was also used to compute the effective stresses in each slice, which was used to compute the microstresses. However, in this model Poisson effects were neglected in the micromechanics, and the analyses assumed that the material had an elastic, strain rate independent deformation. Goldberg extended this slicing approach in order to include material nonlinearity and strain rate dependency in the deformation analysis of carbon fiber reinforced polymer matrix composites.[11,12] This advanced micromechanics model was implemented into classical laminated plate theory for the analysis of symmetric thin laminated plates subject to in-plane loading.[13] In this work, several key issues which are important in the mechanical analysis of composite laminated plates under impact loading were considered. However, transverse shear stresses and strains, which are also important in the analysis of impact problems, were neglected.

In the present paper, first the inelastic constitutive model used to model the nonlinear, strain rate dependent deformation of the polymer matrix constituent will be briefly described. Next, the previously developed micromechanics model[12] will be extended to incorporate the effects of transverse shear stresses and strains into the strain rate dependent inelastic composite analyses. Various uniform stress and uniform strain assumptions to be applied to the unit cell will be investigated, and the resulting formulation will be validated through comparisons to closed form analytical and finite element results. Revisions to the micromechanics method to allow for the computation of through the thickness strain and transverse Poisson's ratios will be presented. Finally, the implementation of the revised micromechanics model into a refined HOT, in order to improve the ability of the methodology to analyze polymer matrix composites

subjected to impact loadings, will be presented and some sample numerical calculations on a representative polymer matrix composite will be discussed.

Constitutive Equations to Analyze Nonlinear Deformation of Polymer Matrix Constituent

To analyze the nonlinear, strain rate dependent deformation of the polymer matrix constituent, the Bodner-Partom viscoplastic state variable model,[14] which was originally developed to analyze the viscoplastic deformation of metals above one-half of the melting temperature, has been modified.[11] In state variable models, a single unified strain variable is defined to represent all inelastic strains.[15] Furthermore, in the state variable approach there is no defined yield stress. Inelastic strains are assumed to be present at all values of stress, the inelastic strains are just assumed to be very small in the "elastic" range of deformation. State variables, which evolve with stress and inelastic strain, are defined to represent the average effects of the deformation mechanisms.

In the modified Bodner model used in this study, the components of the inelastic strain rate tensor, $\dot{\varepsilon}_{ij}^{I}$, are defined as a function of the deviatoric stress components S_{ij}, the second invariant of the deviatoric stress tensor J_2 and an isotropic state variable Z, which represents the resistance to molecular flow. The components of the inelastic strain rate are defined as follows

$$\dot{\varepsilon}_{ij}^{I} = 2D_0 \exp\left[-\frac{1}{2}\left(\frac{Z}{\sigma_e}\right)^{2n}\right]\left(\frac{S_{ij}}{2\sqrt{J_2}} + \alpha\delta_{ij}\right) \tag{1}$$

where D_0 and n are both material constants, with D_0 representing the maximum inelastic strain rate and n controlling the rate dependence of the material. The effective stress, σ_e, is defined as

$$\sigma_e = \sqrt{3J_2} + \sqrt{3}\alpha\sigma_{kk} \tag{2}$$

where α is a state variable controlling the level of the hydrostatic stress effects and σ_{kk} is the summation of the normal stress components which equals three times the mean stress. The inelastic strains are added to the elastic strain tensor to obtain the total strains.

The rate of evolution of the internal stress state variable Z and the hydrostatic stress effect state variable α are defined by the equations

$$\dot{Z} = q(Z_1 - Z)\dot{e}_e^I \tag{3}$$

$$\dot{\alpha} = q(\alpha_1 - \alpha)\dot{e}_e^I \tag{4}$$

where q is a material constant representing the "hardening" rate, and Z_1 and α_1 are material constants representing the maximum value of Z and α, respectively. The initial values of Z and α are defined by the material constants Z_0 and α_0. The term $\dot{e}_e^I$ in equations (3) and (4) represents the effective deviatoric inelastic strain rate, which is defined as

$$\dot{e}_e^I = \sqrt{\frac{2}{3}\dot{e}_{ij}^I \dot{e}_{ij}^I}$$
$$\dot{e}_{ij}^I = \dot{\varepsilon}_{ij}^I - \dot{\varepsilon}_m^I \delta_{ij} \tag{5}$$

where $\dot{\varepsilon}_{ij}^I$ are the components of the inelastic strain rate tensor and $\dot{\varepsilon}_m^I$ is the mean inelastic strain rate. In many state variable constitutive models developed to analyze the behavior of metals,[15] the total inelastic strain and strain rate are used in the evolution laws and are assumed to be equal to their deviatoric values. As discussed by Li and Pan,[16] since hydrostatic stresses contribute to the inelastic strains in polymers, indicating volumetric effects are present, the mean inelastic strain rate cannot be assumed to be zero, as is the case in the inelastic analysis of metals. Further information on the constitutive model, along with the procedures required to obtain the material constants, can be found in Goldberg, et al.[11]

Modification of Micromechanics Model to Include Effects of Transverse Shear Deformation

To compute the effective strain rate dependent, nonlinear deformation response of polymer matrix composites based on the response of the individual constituents, a micromechanical model has been developed.[12] In this model, the unit cell is defined to consist of a single fiber and its surrounding matrix. The composite laminates are assumed to have a periodic, square fiber packing and a perfect interfacial bond. Due to symmetry, only one-quarter of the representative unit cell is analyzed. The fiber is assumed to be transversely isotropic, linear elastic and rate independent (common assumptions for carbon fibers) with a circular cross section. The matrix is assumed to be isotropic with a rate dependent, nonlinear deformation response computed using the equations described in the previous section. The unit cell is divided into several rectangular, horizontal slices of equal thickness as shown in figure1. Due to symmetry, only one-quarter of the unit cell needs to be analyzed. All slices are assumed to be in a plane stress state, i.e., only in-plane strains and stresses are considered. Each slice then is separated into two subslices, one composed of fiber material and the other composed of matrix material. Along the fiber direction (direction 1), the strains are assumed to be equal in each subslice of the slice, and the stresses are combined using volume averaging. The in-plane transverse normal stresses (direction 2) and in-plane shear stresses (direction 12) are assumed to be equal in each subslice of the slice, and the strains are combined using volume averaging. Likewise, all the average strains in each slice are assumed to be equal, and the stresses are combined using volume averaging. The out-of-plane normal strains (direction 3) are assumed to be uniform in each slice, and the volume average of the out-of-plane stresses in each subslice is assumed to be zero. The effective properties, stresses and strains for each slice are computed by applying these assumptions along with the constitutive equations for the fiber and matrix and solving the resulting series of equations. The equivalent stresses, strains and properties for the unit cell can then be computed by applying laminate theory to each slice. The advantage of this type of modeling approach over other micromechanics methods is that the behavior of each slice is decoupled, and the response of each slice can be determined independently. This process results in a series of small matrix equations, instead of one large system of equations, which reduces the complexity of the analysis significantly and increases the computational efficiency. For elastic materials, the property of transverse isotropy of the material could be maintained by using a combination of horizontal and vertical slices and the concept of superposition.[9] However, for the nonlinear materials used in this study, superposition cannot be applied, and due to the fact that only horizontal slicing is used, the inherent transverse isotropy of the composite unit cell is lost. Furthermore, transverse shear effects were neglected in the original analysis. The goal of the present work is to include the effects of transverse shear deformation in the micromechanics, taking into account the fact that the basic sliced unit cell is not naturally transversely isotropic.

Constitutive Models for Fiber and Matrix for Transverse Shear Analysis

In the development of the revised micromechanics model in which transverse shear effects are included, once again the fibers are assumed to be linear elastic and rate independent, and the nonlinear, rate dependent behavior of the polymer matrix is computed using the constitutive equations described earlier. The constitutive relationships of transverse shear deformation (direction 13 and 23) for the fiber and matrix are expressed as

$$\begin{aligned} \gamma^F &= \left(1/G_f\right)\sigma^F \\ \gamma^M &= \left(1/G_m\right)\sigma^M + \gamma^{MI} \end{aligned} \tag{6}$$

where γ^F and γ^M represent the transverse shear strains of the fiber and matrix, respectively, γ^{MI} represents the inelastic transverse shear strain in the matrix, and σ^F and σ^M represent the transverse shear stresses of the fiber and matrix, respectively. G_f and G_m represent the transverse shear modulus of the fiber and matrix, respectively. Note that the general form of the equations is the same whether the 13 direction or 23 direction transverse shear stresses and strains are considered. The only difference would be in which shear modulus (13 or 23) for the fiber is used in the equations.

Different Unit Cell Assumptions for Computing Transverse Shear Deformation

In this paper, four possible assumptions are chosen for the unit cell in order to compute the local and effective transverse shear deformation of the composite ply. To achieve an acceptable level of accuracy in the calculations while maintaining a reasonable level of computational efficiency, several relatively simple sets of assumptions are proposed and investigated in this work. The various sets of assumptions are investigated to determine which result in the most accurate answers. The basic idea of all of these assumptions is to assume either a uniform stress distribution or a uniform strain distribution within each slice and either the average strain or average stress of each slice is equal in the unit cell. For the slices that are composed of both fiber and matrix, two possible assumptions of transverse shear deformation can be made in each slice. These are as follows.

1. The strains are constant within the slice *i* and the stresses within the slice are combined using volume averaging, that is

$$\begin{aligned} \gamma^i &= \gamma^{iF} = \gamma^{iM} \\ \sigma^i &= V_f^i \sigma^{iF} + \left(1 - V_f^i\right)\sigma^{iM} \end{aligned} \tag{7}$$

where V_f^i is the local fiber volume fraction within slice *i*. γ^j and σ^i represent the equivalent transverse strain and stress of slice *i*, respectively. γ^{jF} and σ^{iF} represent the equivalent transverse strain and stress in the fiber within slice *i*, and γ^{jM} and σ^{iM} represent the equivalent transverse strain and stress in the matrix within slice *i*. Substituting eq. (6) into eq. (7), the following expression of the equivalent transverse stress in slice *i* in terms of the equivalent transverse strain in slice *i* and the transverse inelastic strain of matrix is obtained

$$\sigma^i = \left(V_f^i G_f + \left(1 - V_f^i\right)G_m\right)\gamma^i - \left(1 - V_f^i\right)G_m\gamma^{iMI} \tag{8}$$

where once again the equation is valid for both 13 and 23 direction stresses and strains.

2. The stresses are constant within the slice *i* and the strains are combined using volume averaging, that is

$$\begin{aligned} \sigma^i &= \sigma^{iF} = \sigma^{iM} \\ \gamma^i &= V_f^i \gamma^{iF} + (1 - V_f^i)\gamma^{iM} \end{aligned} \tag{9}$$

From eqs. (6) and (9), the following expression for the equivalent transverse strain of slice *i* in terms of equivalent transverse stress for slice *i* and the inelastic strain of the matrix is obtained

$$\gamma^i = \left(V_f^i / G_f + \left(1 - V_f^i\right) / G_m\right)\sigma^i + \left(1 - V_f^i\right)\gamma^{iMI} \tag{10}$$

Similarly, two possible assumptions on the transverse shear deformation between the slices of the unit cell are investigated.

1. The strains are constant between slices and the stresses are combined using volume averaging, that is

$$\begin{aligned} \gamma &= \gamma^i \\ \sigma &= \sum_i h_f^i \sigma^i, \quad i = 1 \cdots N_f + 1 \end{aligned} \tag{11}$$

In eq. (11), γ and σ represent the equivalent transverse shear strain and equivalent transverse shear stress of the unit cell, respectively. N_f represents the number of fiber slices in the quarter of the unit cell which is analyzed, and h_f^i represents the ratio of the thickness of slice *i* to the total thickness of the unit cell.[12]

1. The stresses are constant between slices and the strains are combined using volume averaging, that is

$$\begin{aligned} \sigma &= \sigma^i \\ \gamma &= \sum_i h_f^i \gamma^i, \quad i = 1 \cdots N_f + 1 \end{aligned} \tag{12}$$

Equations (8), (10), (11) and (12) result in four possible combinations of assumptions to describe the transverse shear deformation of the composite unit cell. Table 1 presents the equivalent transverse shear modulus *G* and equivalent inelastic transverse shear strains γ' of the unit cell resulting by applying the various assumptions. These assumptions are denoted by assumption (1) to (4) in this table in order to uniquely identify them.

Numerical Investigation of Effective Transverse Shear Modulus Resulting From Assumptions

As shown in table 1, each of the various combinations of assumptions both within the slice and between slices can result in significantly different effective transverse shear moduli. To investigate qualitatively the differences in effective shear moduli that result by applying the different assumptions, a series of numerical computations are performed. In the next section, specific quantitative verification studies will be carried out to determine which set of assumptions most accurately predicts the composite transverse shear modulus, and by extension the transverse shear response of the composite.

The first qualitative analysis is shown in Table 2. In this table, the values of the nondimensionalized transverse shear modulus of the unit cell computed using the different assumptions is shown. The parameters used in this computation are the nondimensionalized shear modulus of fiber, (G_f/G_m), which is set equal to 15.92 (a typical value for carbon fiber reinforced polymer matrix composites), and the fiber volume fraction, V_f, which is equal to 0.6 (again, a typical value). As can be seen in the table, the assumptions which are utilized result in significant differences in the effective shear modulus which is predicted. Assumption (1) (refer to table 1) results in the highest effective shear modulus by a significant amount. The remaining assumptions display some variation in values, with assumption (4) yielding the lowest value. The dependence of the transverse shear modulus on V_f under the various assumptions is shown in figure 2. Figure 2 shows the variation of the nondimensionalized transverse shear modulus of the unit cell, (G/G_m) with V_f under the different assumptions. Note that the maximum V_f is 0.785 (a maximum possible fiber volume fraction for a square pack fiber architecture) and that these figures are plotted with a value of (G_f/G_m) = 15.92. The various assumptions used are denoted (1) to (4) as indicated in table 1. As seen from figure 2, assumption (1) consistently yields the stiffest modulus, and the variation of modulus with fiber volume fraction is linear. The other assumptions yield a nonlinear variation of effective shear modulus with fiber volume fraction. Assumption (4) consistently yields the softest modulus, and the curves generated by using assumptions (2) and (3) fall in between. The maximum deviation between assumption (1) and the remaining assumptions occurs at $V_f = 0.6$. However, at higher volume fractions the differences between the results generated by assumptions (2)-(4) become more pronounced, with the maximum difference occurring at $V_f = 0.785$. Figure 3 presents the variation in (G/G_m) with (G_f/G_m) under the various assumptions, for a constant volume fraction V_f of 0.6. From this figure, it appears that, for assumptions (2) to (4), the change in effective shear modulus as a function of fiber modulus is not very significant, particularly for higher values of the fiber shear modulus. Assumption (1) yields a linear increase with increasing fiber modulus. To provide a more general representation of the results discussed above, figures 2 and 3 are plotted on the surface of (G/G_m) ~ [(G_f/G_m), V_f], as shown in figure 4. From these figures, it can be seen that the various assumptions on the composite unit cell yield significant differences in the computed effective transverse shear modulus.

Verification of Assumptions of Transverse Shear Deformation

As shown in the previous section, by applying different uniform stress and uniform strain assumptions to the composite unit cell, both within slices and between slices, significant variations in the computed effective transverse shear modulus result. Therefore, it is important to determine which assumption yields the most accurate answers in computing the transverse deformations in the 13 and 23 directions. As discussed earlier, this task is complicated by the fact that the slicing methodology employed in this work eliminates the inherent transverse isotropy present in the unit cell. Therefore, the appropriate assumptions to use in the transverse shear analysis are determined by comparing the equivalent shear modulus computed using the micromechanics method described here (including the various assumptions) and modulus values computed using alternative theoretical and numerical methods. There are some existing models which can be used to verify these assumptions. A very well known model, derived by Hill[17] and Hashin,[18] is used to verify and examine the transverse shear assumptions in the 13 direction. To verify and examine the transverse shear assumptions in the 23 direction, the commercial finite element software ABAQUS[19] is used to compute the transverse shear modulus.

Model for Computing Transverse Shear Modulus in 23 Direction in ABAQUS

Considering the transverse isotopic properties of the unit cell, the model for conducting the transverse shear modulus analysis in ABAQUS[19] is reduced to a two-dimensional model. In this procedure, one or multiple unit cells are used to calculate the equivalent transverse shear modulus of the unit cell. The

elastic constants of the fiber and matrix used in these analyses are shown in table 3, which are representative properties for a carbon fiber reinforced polymer matrix composite system and are taken from Goldberg, et al.[11, 12] The adequacy of the mesh size is verified via comparison of the results obtained by varying the mesh density. When $V_f \leq 0.6$, one unit cell is divided into 1600 plane strain elements; and when $V_f = 0.7$, 10000 plane strain elements are used in the calculations.

When calculating the transverse shear modulus of the unit cell, it is crucial to apply appropriate boundary conditions to account for the influence of surrounding unit cells. Determining the boundary conditions prior to computation is quite difficult because the edges of unit cell do not remain straight during shear deformation. In this paper, an approximate approach is developed by using "stress boundary loading" and "strain boundary loading" conditions as shown in figure 5. In stress boundary loading, the edges of the unit cell are subjected to tangential displacement loadings (analogous to adding stress loading) and the displacements normal to the edges are not constrained. It is important to note that this definition does not imply maintaining constant stresses. When strain boundary loading is applied, the edges of the unit cell are subjected to combinations of tangential and normal displacement loadings so that the deformed shape of the model is a parallelogram. Once again, this does not imply maintaining constant strain. In computing the transverse shear modulus, firstly, the stress and strain are calculated at the centroid of each element. Then these stresses and strains are combined using volume averaging to obtain the average stress and strain, respectively. The effective transverse shear modulus G_{23} is calculated by using the following expression.

$$G_{23} = \frac{\sum_i \sigma_{23i} V_i \Big/ \sum_i V_i}{\sum_i \varepsilon_{23i} V_i \Big/ \sum_i V_i} \tag{13}$$

where the summation is over the elements i, V_i is the volume of element i, σ_{23i} is the transverse shear stress in element i and ε_{23i} is the transverse shear strain in element i.

Figure 6 illustrates the procedure used to obtain an accurate value of G_{23}. At first, by applying stress boundary loading on one unit cell, the transverse shear modulus G_{23}^{1s} is obtained. Then by applying stress boundary loading on an assemblage of nine unit cells arranged in a three by three pattern, G_{23}^{2s} calculated from the central unit cell is obtained. By applying stress boundary loadings on a larger assemblages of unit cells (five by five, seven by seven, etc.), a series of effective transverse shear moduli, $G_{23}^{1s}, G_{23}^{2s}, G_{23}^{3s}, \cdots G_{23}^{ns}$, are obtained (as shown in fig. 6). As the number of unit cells is increased, the computed transverse shear modulus increases. Similarly, by applying strain boundary loadings to a series of increasingly larger assemblages of unit cells, a series of effective transverse shear moduli, $G_{23}^{1e}, G_{23}^{2e}, G_{23}^{3e}, \cdots G_{23}^{ne}$, which decrease in magnitude as more unit cells are used, are obtained. When n is large enough, while not explicitly shown in Figure 6, $G_{23}^{ns} \approx G_{23}^{ne} \approx G_{23}$, resulting in a converged effective transverse shear modulus of the unit cell.

Numerical results obtained using this procedure is presented in figure 7. The composite material S2 Glass/Epoxy, with fiber volume fraction 0.6, is used here. This material was chosen since the glass fiber is isotropic, which simplifies the analysis. For this material, both the fiber and matrix materials in this composite are isotropic. The shear moduli of Glass and Epoxy are 35.04 GPa and 1.53 GPa, respectively. Results in figure 7 show that convergence is obtained using an assemblage of three by three unit cells. It can be seen that by applying stress boundary conditions to a unit cell, a value of G_{23}^{1s} almost equal to the converged multi unit-cell model, G_{23}, is obtained. The error is on the order of 0.5 percent, which is very small compared to the differences in shear modulus values resulting from the different assumptions. Due

to this small difference (between G_{23}^{1s} and G_{23}), the stress controlled unit cell value of G_{23}^{1s} is used to conduct the analysis described in the following section.

Model for Computing Transverse Shear Modulus in 13 Direction

A solution based on a cylinders model, assuming that the fiber phase is composed of infinitely long circular cylinders embedded in a continuous matrix phase, was developed by Hill[17] and Hashin.[18] An exact solution of the displacement field was obtained and the equivalent transverse shear modulus in the 13 direction for the fiber reinforced material was expressed as follows.

$$G_{13} = G_m\left[G_{12f}(1+V_f) + G_m(1-V_f)\right] \Big/ \left[G_{12f}(1-V_f) + G_m(1+V_f)\right] \tag{14}$$

where G_{12f} and G_m are the shear modulus of the fiber and matrix, respectively, and V_f is the fiber volume fraction of the unit cell. It must be noted that the unit cell model developed in this work is different from that due to Hill[17] and Hashin.[18] However, from a macroscopic point of view, both models result in the same equivalent transverse shear modulus for a laminated composite. Thus the results obtained using eq. (14) can be used to verify the assumptions discussed earlier. The quantitative analyses and determination of the appropriate assumptions to use will be discussed in a later section of the article.

Study on Through the Thickness Strains and Transverse Poisson's Ratio

To accurately compute the through thickness behavior of polymer matrix composites under impact loading, modeling through the thickness strains and the transverse Poisson's ratio become important. In the current work, the micromechanics model developed by Goldberg,[12] which did not address these issues, is further extended to compute these values.

Based on the original work reported by Goldberg,[12] each slice in figure 1 is analyzed independently. Most of the slices are assumed to have two subslices, with the exception of the top slice. One subslice represents fiber material and the other subslice represents matrix material. The top slice is assumed to comprise matrix material only. The micromechanics equations presented here are for those slices composed of both fiber and matrix material. The stresses in the slices comprising pure matrix can be computed using the matrix elastic properties and inelastic constitutive equations (eqs.(1) to (5)) directly. The transversely isotropic and isotropic compliance matrices are used to relate the local strains to the local stress in the fiber and matrix using the following relations.

$$\begin{Bmatrix} \varepsilon_{11}^F \\ \varepsilon_{22}^F \\ \varepsilon_{33}^F \end{Bmatrix} = \begin{bmatrix} S_{11f} & S_{12f} & S_{12f} \\ S_{12f} & S_{22f} & S_{23f} \\ S_{12f} & S_{23f} & S_{22f} \end{bmatrix} \begin{Bmatrix} \sigma_{11}^F \\ \sigma_{22}^F \\ \sigma_{33}^F \end{Bmatrix} \tag{15}$$

$$\begin{Bmatrix} \varepsilon_{11}^M \\ \varepsilon_{22}^M \\ \varepsilon_{33}^M \end{Bmatrix} = \begin{bmatrix} S_{11m} & S_{12m} & S_{12m} \\ S_{12m} & S_{11m} & S_{12m} \\ S_{12m} & S_{12m} & S_{11m} \end{bmatrix} \begin{Bmatrix} \sigma_{11}^M \\ \sigma_{22}^M \\ \sigma_{33}^M \end{Bmatrix} + \begin{Bmatrix} \varepsilon_{11}^{IM} \\ \varepsilon_{22}^{IM} \\ \varepsilon_{33}^{IM} \end{Bmatrix} \tag{16}$$

where the stresses, $\sigma_{ij,}$ and strains, $\varepsilon_{ij,}$ are defined in a Cartesian frame of reference and S_{ij} represent terms in the material compliance matrix. A superscript "*I*" is used to denote inelastic strains and superscripts "*F*" and "*M*" are used to indicate fiber subslice and matrix subslice, respectively. Subscripts "*f*" and "*m*"

refer to fiber and matrix related properties, respectively. Out-of-plane normal stresses are included in the analysis since although each slice is assumed to be in a state of global plane stress, the individual subslices are assumed to be in a full three-dimensional state of stress. The relationships between shear stresses and shear strains are not presented here because the through the thickness strain and transverse Poisson's ratio are independent of these quantities.

Based on the slice geometry (fig. 1), slice fiber volume fraction and the basic definitions governing displacement and force equilibrium, the uniform stress and uniform strain assumptions used for the micromechanics model can be stated as

$$\begin{aligned}
\varepsilon^i_{11f} &= \varepsilon^i_{11m} = \varepsilon^i_{11} \\
\varepsilon^i_{22} &= V^i_f \varepsilon^i_{22f} + (1 - V^i_f)\varepsilon^i_{22m} \\
\varepsilon^i_{33f} &= \varepsilon^i_{33m} = \varepsilon^i_{33} \\
\sigma^i_{11} &= V^i_f \sigma^i_{11f} + (1 - V^i_f)\sigma^i_{11m} \\
\sigma^i_{22f} &= \sigma^i_{22m} = \sigma^i_{22} \\
\sigma^i_{33} = 0 &= V^i_f \sigma^i_{33f} + (1 - V^i_f)\sigma^i_{33m}
\end{aligned} \tag{17}$$

where the superscript i represents variables related to slice i.

Combining the uniform stress and uniform strain assumptions (eq. (17)) with the constituent stress-strain relations (eqs. (15) and (16)), the stress variables, σ^{iF}_{11}, σ^{iM}_{11}, σ^{iF}_{33}, σ^{iM}_{33} and σ^i_{22} can be derived in terms of the total and inelastic strains in the 1 and 2 directions as follows

$$\begin{aligned}
\sigma^{iF}_{11} &= Q^{iA}_{11}\varepsilon^i_{11} + Q^{iA}_{12}\varepsilon^i_{22} + \varepsilon^{iAI}_1 \\
\sigma^{iM}_{11} &= Q^{iB}_{11}\varepsilon^i_{11} + Q^{iB}_{12}\varepsilon^i_{22} + \varepsilon^{iBI}_1 \\
\sigma^i_{22} &= Q^i_{21}\varepsilon^i_{11} + Q^i_{22}\varepsilon^i_{22} + \varepsilon^{iI}_2 \\
\sigma^{iF}_{33} &= Q^{iA}_{31}\varepsilon^i_{11} + Q^{iA}_{32}\varepsilon^i_{22} + \varepsilon^{iAI}_3 \\
\sigma^{iM}_{33} &= Q^{iB}_{31}\varepsilon^i_{11} + Q^{iB}_{32}\varepsilon^i_{22} + \varepsilon^{iBI}_3
\end{aligned} \tag{18}$$

where Q^i are the effective stiffness matrix terms and the various ε^{iI} are collections of the inelastic strain terms.[12] Combining eqs. (17) and (18), the following expression for the out-of-plane normal strain in slice i can be expressed (in terms of the computed coefficients H^i) as follows.

$$\varepsilon^i_{33} = H^i_{11}\varepsilon_{11} + H^i_{12}\varepsilon_{22} + \varepsilon^{iI}_3 \tag{19}$$

where ε^{iI}_3 represents collected inelastic strain terms of slice i. Similar expressions can be derived for the slices containing matrix only. Since the normal stresses in the 3 direction are assumed to be constant (zero) through the thickness direction, the through the thickness normal strain, ε_{33}, is obtained by combining the effective strain values at each slice (eq. (19)) using the following expression.

$$\varepsilon_{33} = \sum_{i=1}^{N_f+1} h^i_f \varepsilon^i_{33} \tag{20}$$

In eq. (20), h_f^i is the thickness ratio for slice *i,* which is defined as h^i/h^T , where h^i is the thickness of slice *i*, h^T is the total thickness of the quarter of the unit cell which is analyzed and N_f is related to the number of fiber slices as mentioned before. Substitution of eq. (19) into eq. (20) yields the following.

$$\varepsilon_{33} = H_{11}\varepsilon_{11} + H_{12}\varepsilon_{22} + \varepsilon_3^I \tag{21}$$

where

$$\begin{aligned} H_{11} &= \sum_{i=1}^{N_f+1} h_f^i H_{11}^i \\ H_{12} &= \sum_{i=1}^{N_f+1} h_f^i H_{12}^i \\ \varepsilon_3^I &= \sum_{i=1}^{N_f+1} h_f^i \varepsilon_3^{iI} \end{aligned} \tag{22}$$

To determine the effective inelastic strain in the through thickness direction $\left(\varepsilon_{33}^I\right)$, eq. (21) is rearranged as

$$\varepsilon_{33} = H_{11}\left(\varepsilon_{11} - \varepsilon_{11}^I\right) + H_{12}\left(\varepsilon_{22} - \varepsilon_{22}^I\right) + \varepsilon_{33}^I \tag{23}$$

Using eqs. (20) and (21), the inelastic normal strain can be expressed as follows.

$$\varepsilon_{33}^I = H_{11}\varepsilon_{11}^I + H_{12}\varepsilon_{22}^I + \varepsilon_3^I \tag{24}$$

To determine the transverse Poisson's ratios, the procedure proposed by Whitney[9] is used. Equation (21) is simplified for elastic loading along two directions. First, for loading along the 1 direction, using the usual definition for Poisson's ratio, ν , the following equation is obtained.

$$-\nu_{13}\varepsilon_{11} = H_{11}\varepsilon_{11} - \nu_{12}H_{12}\varepsilon_{11} \tag{25}$$

which can be simplified to yield the following expression

$$\nu_{13} = -H_{11} + \nu_{12}H_{12} \tag{26}$$

Likewise, for loading along the 2 direction, the following result is obtained.

$$-\nu_{23}\varepsilon_{22} = H_{12}\varepsilon_{22} - \nu_{21}H_{11}\varepsilon_{22} \tag{27}$$

which can be simplified to yield

$$\nu_{23} = -H_{12} + \nu_{21}H_{11} \tag{28}$$

Implementation of Higher Order Laminated Plate Theory Into Strain Rate Dependent Micromechanics Model

A micro-macro analysis procedure is developed by coupling the strain rate dependent micromechanical model with a refined HOT. In this procedure, the verified assumptions which appear to provide the best descriptions of the transverse shear deformation, which are discussed in a later section of this article, are used. On the laminate level, the traditional HOT[3,4] is refined to capture the inelastic strain effects. In this work, hydrothermal effects are neglected.

Modified Higher Order Laminated Plate Theory

In the higher order theory, cubic through-the-thickness variations are assumed to describe the inplane deformations and the out of plane deformation is assumed to be independent of laminate thickness. This allows an accurate and efficient description of transverse shear stresses, which are important in anisotropic laminates. The displacement field is expressed as follows.

$$\begin{aligned} u(x,y,z) &= u_0(x,y) + z\phi_x(x,y) + z^2\varphi_x(x,y) + z^3\theta_x(x,y) \\ \upsilon(x,y,z) &= \upsilon_0(x,y) + z\phi_y(x,y) + z^2\varphi_y(x,y) + z^3\theta_y(x,y) \\ w(x,y,z) &= w_0(x,y) \end{aligned} \tag{29}$$

where $u(x,y,z)$, $\upsilon(x,y,z)$, $w(x,y,z)$ are the displacements of a point (x,y,z) and $u_0(x,y)$, $\upsilon_0(x,y)$, $w_0(x,y)$ are the corresponding values in the mid-plane and z is the distance from the mid-plane along the thickness. Application of the stress-free boundary conditions, $\sigma_{13}\big|_{z=\pm h/2} = \sigma_{23}\big|_{z=\pm h/2} = 0$, at top and bottom surfaces, results in the following expressions for strains associated with the displacements, described in eq. (29) .

$$\begin{aligned} \varepsilon_1 &= \varepsilon_1^0 + z\varepsilon_1^1 + z^3\varepsilon_1^3 \\ \varepsilon_2 &= \varepsilon_2^0 + z\varepsilon_2^1 + z^3\varepsilon_2^3 \\ \varepsilon_6 &= \varepsilon_6^0 + z\varepsilon_6^1 + z^3\varepsilon_6^3 \\ \varepsilon_4 &= \varepsilon_4^0 + z^2\varepsilon_4^2 \\ \varepsilon_5 &= \varepsilon_5^0 + z^2\varepsilon_5^2 \end{aligned} \tag{30}$$

where

$$
\begin{aligned}
&\varepsilon_1^0 = \frac{\partial u_0}{\partial x}, \varepsilon_1^1 = \frac{\partial \phi_x}{\partial x}, \varepsilon_1^3 = -\frac{4}{3h^2}\frac{\partial \phi_x}{\partial x} \\
&\varepsilon_2^0 = \frac{\partial \upsilon_0}{\partial y}, \varepsilon_2^1 = \frac{\partial \phi_y}{\partial y}, \varepsilon_2^3 = -\frac{4}{3h^2}\frac{\partial \phi_y}{\partial y} \\
&\varepsilon_6^0 = \frac{\partial u_0}{\partial y} + \frac{\partial \upsilon_0}{\partial x}, \varepsilon_6^1 = \frac{\partial \phi_x}{\partial y} + \frac{\partial \phi_y}{\partial x}, \varepsilon_6^3 = -\frac{4}{3h^2}\left(\frac{\partial \phi_x}{\partial y} + \frac{\partial \phi_y}{\partial x}\right) \\
&\varepsilon_4^0 = \frac{\partial w_0}{\partial x} + \phi_x, \varepsilon_4^2 = -\frac{4}{h^2}\varepsilon_4^0 \\
&\varepsilon_5^0 = \frac{\partial w_0}{\partial y} + \phi_y, \varepsilon_5^2 = -\frac{4}{h^2}\varepsilon_5^0
\end{aligned}
\tag{31}
$$

In eqs. (30) and (31), the strains are expressed using conventional engineering notations (that is, 1 = 11, 2 = 22, 6 = 12, 4 = 23 and 5 = 13) and h represents the plate thickness.

Combining eqs. (30) and (31) and the equivalent constitutive relationship of each ply, the resultant forces are expressed in terms of the mid-plane strains and inelastic resultant forces. For a symmetric laminate, these expressions can be written as follows

$$
\begin{aligned}
&\begin{Bmatrix} N_1 \\ N_2 \\ N_6 \end{Bmatrix} = \begin{bmatrix} A_{11} & A_{12} & A_{16} \\ A_{12} & A_{22} & A_{26} \\ A_{16} & A_{26} & A_{66} \end{bmatrix} \begin{Bmatrix} \varepsilon_1^0 \\ \varepsilon_2^0 \\ \varepsilon_6^0 \end{Bmatrix} - \begin{Bmatrix} {N_1}^I \\ {N_2}^I \\ {N_6}^I \end{Bmatrix} \\
&\begin{Bmatrix} Q_4 \\ Q_5 \end{Bmatrix} = \left(\begin{bmatrix} A_{44} & A_{45} \\ A_{45} & A_{55} \end{bmatrix} - \frac{4}{h^2}\begin{bmatrix} D_{44} & D_{45} \\ D_{45} & D_{55} \end{bmatrix} \right) \begin{Bmatrix} \varepsilon_4^0 \\ \varepsilon_5^0 \end{Bmatrix} - \begin{Bmatrix} {Q_4}^I \\ {Q_5}^I \end{Bmatrix}
\end{aligned}
\tag{32}
$$

where

$$
\begin{aligned}
N_i &= \int_{-h/2}^{h/2} \sigma_i dz && (i = 1,2,6) \\
Q_i &= \int_{-h/2}^{h/2} \sigma_i dz && (i = 4,5) \\
A_{ij} &= \int_{-h/2}^{h/2} \overline{Q}_{ij} dz && (i, j = 1,2,6) \\
\left(A_{ij}, D_{ij}\right) &= \int_{-h/2}^{h/2} \overline{Q}_{ij}\left(1, z^2\right) dz && (i, j = 4,5) \\
N_i^I &= \int_{-h/2}^{h/2} \overline{Q}_{ij} \varepsilon_j^I dz && (i, j = 1,2,6) \\
Q_i^I &= \int_{-h/2}^{h/2} \overline{Q}_{ij} \varepsilon_j^I dz && (i, j = 4,5)
\end{aligned}
\tag{33}
$$

In eqs. (32) and (33), all variables are defined in the structural axis system and conventional engineering notations are used to express normal and shear stresses and strains. The quantities N_i and Q_i are the in-plane force resultants and transverse shear force resultants, respectively and N_i^I and Q_i^I are the inelastic in-plane force resultants and inelastic transverse shear force resultants, respectively. A_{ij} and

D_{ij} are laminate stiffness matrix components and $\overline{Q}_{ij}$, σ_i and ε_j^I are the stiffness matrix components, stresses and the inelastic strains of each ply in the structural axis system, respectively. In this refined HOT, both transverse shear effects and inelastic effects which are important in the impact problem are considered. The in-plane force resultants and transverse shear force resultants are decoupled in a symmetric laminate. It must be noted that the Q used here have a different meaning from those used in eq. (18) which represent the calculated effective stiffness matrix terms of slice i in a unit cell.

Computational Procedure

The details of the computational procedure are illustrated in figure 8, where the left half represents the macro-component of the analysis procedure using the higher order theory (HOT), and the right half describes the micro-component of the analysis based on the extended micromechanics model. First, the mid-plane strains of the laminated plate are obtained from direct input or a finite element program. Then the strains of each layer are calculated using eq. (30). Because each layer is represented by a unit cell, the strains of each layer are transferred into a unit cell in the micro-part of this procedure. In the unit cell, the input strains are used to calculate the stresses of each subslice. Then the inelastic strains of the matrix subslice are calculated using eqs. (1) to (5). This is followed by calculation of the equivalent inelastic strains of the unit cell, which are then transferred back to the macro-part of this procedure. Finally the resultant forces of the laminate are calculated using mid-plane strains of the laminate and the inelastic strains of each layer.

Results

First, numerical analysis is conducted to investigate the validity and accuracy of the different assumptions discussed in the Modification of Micromechanics Model to Include Effects of Transverse Shear Deformation section (table 1). A representative polymer matrix composite material, IM7/977-2, with a fiber volume fraction of 0.6, is used in this study. Detailed convergence studies on N_f was conducted in earlier work.[12] Therefore, in present work, 5 fiber slices ($N_f = 5$) in the quarter of the unit cell are used. The uniform stress and uniform strain assumptions that yield the best values to describe the deformations in the 13 and 23 directions are determined and these are subsequently used in the structural analysis of composite laminated plates. The mechanical behavior of composite plates with various stacking sequence are investigated under various strain rate loadings.

Verification of the Transverse Shear Modulus *G*23 and *G*13

For the verification studies, properties for the carbon fiber reinforced polymer matrix composite system, IM7/977-2, presented by Goldberg, et al.[11,12] were used. The material properties are listed in table 3. Only the elastic transverse shear properties of the fiber and matrix are used here.

Comparison of the effective transverse shear modulus values, G_{23}, obtained using the four assumptions on the unit cell discussed earlier (and shown in table 1) with those obtained using ABAQUS are presented in figure 9. Figure 9 represents the variation in transverse shear modulus G_{23} with V_f (overall composite fiber volume fraction). From this figure, it can be concluded that the results obtained using assumption 3 have a good correlation with those obtained using ABAQUS when the fiber volume fraction is less than 0.3. When V_f is equal to or greater than 0.6, the shear modulus results obtained using assumption 4 show better correlation with ABAQUS. Since the normal range of V_f for composite materials used in impact applications is typically between 0.5 and 0.7, assumption 4 is chosen in this

work. The transverse shear deformation in the 23 direction is obtained by applying this assumption to a unit cell and these values are used in subsequent computations.

The effective transverse shear modulus, G_{13}, obtained using the four assumptions and the values obtained using the formulation from Hill[17] and Hashin[18] (eq.14) are compared in figure 10. As can be seen in the figure, the results obtained using assumption 3 show a good correlation with the results obtained using the closed form formulation. At high volume fractions, due to differing assumptions as to how the unit cell is constructed, there is some deviation between the analytical result and the values computed using the micromechanics model. Since the fiber volume fractions of greatest interest for impact applications range between 0.5 and 0.7, assumption 3 is selected to describe the transverse shear deformation in the 13 direction.

Mechanical Response of Various Laminate Plates Under Different Strain Rate Loadings

In this work, IM7/977-2 composite laminated plates with various stacking sequences are used to investigate the material response under various loading directions and various strain rate loadings. The thicknesses of all the laminates considered are 0.01 m. Material properties of the fiber and matrix are shown in table 3. The fiber is assumed to be linear elastic and the matrix is modeled using the rate dependent, nonlinear model and material properties summarized earlier in this article and described in detail in Goldberg, et al.[11] The composite material has a fiber volume fraction of 0.6. Five fiber slices are used ($N_f = 5$) in the quarter of the unit cell which is analyzed. Assumptions (3) and (4), which appear to provide reasonable descriptions of the transverse shear deformation in the 13 and 23 directions, respectively, are used. Here, directions 1, 2 and 3 represent the material coordinate system and directions x,y and z represent the laminate coordinate system. Subscripts x and y represent in-plane directions and z represents the out-of-plane direction. Thus, for the unidirectional composite plate (stacking sequence [0]), the material axis system coincides with the structural axis system.

The mechanical response of a composite plate with $[0]_4$ stacking sequence is shown in figure 11. This figure represents different stress-strain curves under different strain rate uniaxial loadings in the x, y, xz and yz directions. The experimental values (scatter points) in figure 11b and 12a were taken from Goldberg, et al.[11] The high strain rate testing was conducted using a Hopkinson bar and the low strain rate testing was conducted using an Instron machine. In figure 11(b), the apparent nonlinearity in the experimental high strain rate stress-strain curve along the y direction, and the difference between the experimental and computed results at the high strain rate, is most likely due to the lack of stress equilibrium in the experiments at low strains and the specimen geometry used for the experimental tests. More details regarding the experimental procedures and results are provided in Goldberg et al.[11] Unfortunately, the experimental values were limited to in-plane directions only. The significance of strain rate effects is investigated by studying the effects on the transverse shear stress-strain curves. More experiments along the transverse directions will be conducted in the future. Figure 11(b) and figure 12(a) (discussed later) show good correlations between the experimental values and the computational results under various stacking sequences and various strain rate loadings. Although, the comparisons are based on limited available experimental values, some meaningful observations can still be made regarding the accuracy of the modeling technique. Based on these comparisons, it appears that the developed micro-macro mechanical framework can accurately describe the structural behavior of rate dependent composite laminated plates under various strain rate loadings. From figure 11, it can be seen that almost no strain rate effect is exhibited along the fiber direction, as expected. However significant rate dependencies in the y, xz and yz directions are observed. The stresses increase with an increase in strain rate. Physically, this is due to the fact that in these directions the response of the matrix plays a more dominant role in the stress analysis. In case of the unidirectional laminate, since the material axis and the structural axis coincide, this material rate dependent behavior is reflected in the laminate stresses (in y, xz and yz directions). An important observation is the fact that the magnitudes of the transverse shear stresses are nontrivial. The magnitude of the transverse stresses will also increase with an increase in laminate

thickness. Thus, nontrivial, nonlinear and rate dependent transverse shear stresses, which are important for an impact problem, are observed by using the new modeling techniques. Therefore, it is expected that the developed refined micro-macro mechanical model, which includes transverse shear deformation, will significantly improve the level of accuracy in the impact analysis of composite laminates.

The mechanical response of a composite plate with a $[45]_4$ stacking sequence under uniaxial loadings along x and xz directions is shown in figure 12. Significant rate dependency can be observed both in the normal and in the transverse shear directions. This is because, in case of an orthotropic laminate, the applied loading can be decomposed into loading along the fiber direction and loading along the in-plane transverse normal and shear directions. The loading along fiber direction will not exhibit strain-rate dependency. However, the stresses in the in-plane transverse normal and shear directions will exhibit significant differences under different strain rate loadings. This combined effect results in the rate dependency shown in figure 12 for the $[45]_4$ laminate. These results indicate that along with the material properties of the laminate being considered, plate geometry, stacking sequence and loading directions will also influence the rate dependency in the structural response of composite laminated plates.

Figure 13 shows the mechanical response along xz and yz directions of a composite plate with a [90/0]s stacking sequence. It can be seen that the transverse shear responses are different along the two directions. This can be explained as follows. In HOT, the assumed inplane displacements (u, v) are cubic functions of the thickness coordinate, which results in parabolic distributions of transverse shear strain along the thickness direction. Therefore, in transverse shear stress analysis, the layers closer to mid-plane play a more important role than those near the top and bottom surfaces. This result in different values of 'average' transverse shear moduli of the laminate along yz and xz directions. As a result, the stress-strain curves are different along the two directions. If FSDT is used, due to the linear distribution of displacements (u, v), the transverse shear strains remain constant through the thickness. Therefore, the locations of the layers do not affect the transverse shear stress analysis. As a result, in the case of a cross-ply laminate, the effects shown in figure 13 cannot be observed using FSDT.

Conclusion

An investigation on the nonlinear responses of polymer composite laminate plates under different strain rate loadings is conducted. A strain rate dependent micromechanics model is further extended to account for the transverse shear effects that are important in the impact problem. Four different assumptions of transverse shear deformation are investigated to improve the developed strain rate dependent micromechanics model. Theoretical and finite element investigations are conducted to validate these assumptions. Two of these assumptions are found to be adequate in describing the transverse shear deformation along the transverse directions, over the normal range of fiber volume fraction. Based on these assumptions, a method to determine through the thickness strain and transverse Poisson's ratio is developed. A higher order laminated plate theory, which can capture the through-the-thickness transverse shear stresses, is extended to include inelastic effects and is used in the laminate analysis. An integrated micro-macro numerical procedure is developed by implementing the revised micromechanics model into the refined higher order laminated plate theory, which now contains the inelastic strain effects. The mechanical response of IM7/977-2 composite laminate plates with different stacking sequences are investigated under various strain rate loading conditions. The results illustrate the significant strain rate dependency and nonlinear effects even for moderate strain rate loadings. The strain rate dependency is also influenced by laminate geometry and ply stacking sequence. The results show that transverse shear stresses play an important role at both macro and micro level behavior of composites. In particular, these effects cannot be neglected in the impact analysis of composites laminates.

References

[1]Reddy, J.N., "Mechanics of Laminated composite Plates: Theory and Analysis", CRC Press, 1997.

[2]Whitney, J.M., "The Effect of Transverse Shear Deformation in the Bending of Laminated Plates," Journal of Composite Materials, vol. 3, pp. 534–547, 1969.

[3]Reddy, J.N., "A Simple Higher-Order Theory for Laminated Composite Plates," Journal of Applied Mechanics, vol. 51, no. 4, 1984, pp. 745–752.

[4]Chattopadhyay, A. and Gu H., "New Higher-Order Plate Theory in Modeling Delamination Buckling of Composite Laminates," AIAA Journal, vol. 32, no. 8, 1994, pp. 1709–1716.

[5]Aboudi, J.A., "Micromechanical Analysis of Composites by the Method of Cells," Applied Mechanics Review, vol.42, pp. 193–221, 1989.

[6]Pindera, M.-J. and Bednarcyk, B.A., "An efficient implementation of the generalized method of cells for unidirectional, multi-phased composites with complex microstructures," Composites: Part B, vol.30, pp.87–105, 1999.

[7]Sun, C.T. and Chen, J.L., "A Micromechanics Model for Plastic Behavior of Fibrous Composites," Composites Science and Technology, vol.40, pp. 115–129, 1991.

[8]Robertson, D.D. and Mall, S., "Micromechanical Relations for Fiber-Reinforced Composites Using the Free Transverse Shear Approach," Journal of Composites Technology and Research, vol.15, pp.181–192, 1993.

[9]Whitney, J.M., "A Laminate Analogy for Micromechanics," Proceedings of the American Society for Composites Eighth Technical Conference, G.M. Newaz, ed., Technomic Publishing Co., Lancaster, PA, 1993, pp. 785–794.

[10]Mital, S.K., Murthy, P.L.N., and Chamis, C.C., "Micromechanics for Ceramic Matrix Composites Via Fiber Substructuring," Journal of Composite Materials, vol. 29, pp. 614–633, 1995.

[11]Goldberg R.K., Roberts, G.D. and Gilat, A., "Implementation of an Associative Flow Rule Including Hydrostatic Stress Effects Into the High Strain Rate Deformation Analysis of Polymer Matrix Composites," NASA/TM-2003-212382, National Aeronautics and Space Administration, Washington, D.C., 2003.

[12]Goldberg, R.K., "Implementation of Fiber Substructuring Into Strain Rate Dependent Micromechanics Analysis of Polymer Matrix Composites," NASA/TM—2001-210822, National Aeronautics and Space Administration, Washington, D.C., 2001.

[13]Goldberg, R.K., "Implementation of Laminate Theory Into Strain Rate Dependent Micromechanics Analysis of Polymer Matrix Composites," NASA/TM—2000-210351, National Aeronautics and Space Administration, Washington, D.C., 2000.

[14]Bodner, S.R., "Unified Plasticity for Engineering Applications," Kluwer Academic/Plenum Publishers, New York, 2002.

[15] Stouffer, D.C.; and Dame, L.T., "Inelastic Deformation of Metals. Models, Mechanical Properties and Metallurgy," John Wiley and Sons, New York, 1996.

[16] Li, F.Z; and Pan, J.: "Plane-Stress Crack-Tip Fields for Pressure-Sensitive Dilatant Materials," Journal of Applied Mechanics, vol. 57, pp. 40–49, 1990.

[17]Hill, R., "Theory of Mechanical Properties of Fiber-Strengthened Materials: I. Elastic Behavior," Journal of the Mechanics and Physics of Solids, vol.12 pp.199, 1964

[18]Hashin, Z., "Viscoelastic Fiber Reinforced Materials," AIAA Journal, vol. 4, pp. 1141, 1966

[19]Anonymous, ABAQUS/Standard Users Manual, Version 6.4, ABAQUS, Inc., Pawtucket, RI, 2003.

Table 1.—Formulations under different transverse shear assumptions

Within slice	$\gamma = \gamma^F = \gamma^M$	$\sigma = \sigma^F = \sigma^M$
	$\sigma = V_f \sigma^F + (1-V_f)\sigma^M$	$\gamma = V_f \gamma^F + (1-V_f)\gamma^M$
Between slice	$\sigma^i = \left(V_f^i G_f + \left(1-V_f^i\right)G_m\right)\gamma^i - \left(1-V_f^i\right)G_m \gamma^{iMI}$	$\gamma^i = \left(V_f^i / G_f + \left(1-V_f^i\right)/G_m\right)\sigma^i - \left(1-V_f^i\right)\gamma^{iMI}$
$\gamma = \gamma^i$ $\sigma = \sum_i h_f^i \sigma^i$	$G = \sum_{i=1}^{N_f+1} h_f^i \left(V_f^i G_f + (1-V_f^i)G_m\right)$ $\gamma^I = \sum_{i=1}^{N_f+1} \left(h_f^i (1-V_f^i) G_m \gamma^{iMI}\right) \Big/ G$ Assumption (1)	$G = \sum_{i=1}^{N_f+1} \frac{h_f^i}{V_f^i / G_f + (1-V_f^i)/G_m}$ $\gamma^I = \sum_{i=1}^{N_f+1} \left(\frac{h_f^i (1-V_f^i)\gamma^{iMI}}{V_f^i / G_f + (1-V_f^i)/G_m}\right) \Big/ G$ Assumption (3)
$\sigma = \sigma^i$ $\gamma = \sum_i h_f^i \gamma^i$	$G = \left(\sum_{i=1}^{N_f+1} \frac{h_f^i}{V_f^i G_f + (1-V_f^i)G_m}\right)^{-1}$ $\gamma^I = \sum_{i=1}^{N_f+1} \frac{h_f^i (1-V_f^i) G_m}{V_f^i G_f + (1-V_f^i)G_m} \gamma^{iMI}$ Assumption (2)	$G = \left(\sum_{i=1}^{N_f+1} h_f^i \left(V_f^i / G_f + (1-V_f^i)/G_m\right)\right)^{-1}$ $\gamma^I = \sum_{i=1}^{N_f+1} h_f^i (1-V_f^i)\gamma^{iMI}$ Assumption (4)

Table 2.—Nondimensionalized shear modulus of unit cell under different assumptions

Assumption	G/G_m
1	9.95
2	3.11
3	4.78
4	2.31

Table 3.—Material properties of the fiber and matrix

IM7 fibers								
E11(Gpa)	E22(Gpa)	G12(Gpa)	G23(Gpa)	v12	v23			
276	13.8	20	12.4	0.25	0.25			

977-2 polymer matrix									
$\dot{\varepsilon}$ (/sec)	E(Gpa)	v	Do(/sec)	n	Z_0(Mpa)	Z_1(Mpa)	q	α_0	α_1
9E-5	3.52	0.4	1.00E+06	0.8515	259.496	1131.371	150.498	0.1289	0.15215
1.9	3.52								
500	6.33								

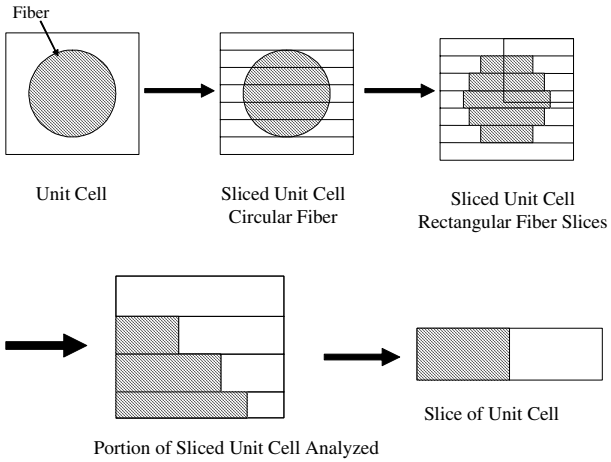

Figure 1. Schematic showing relationship between unit cell and slices.

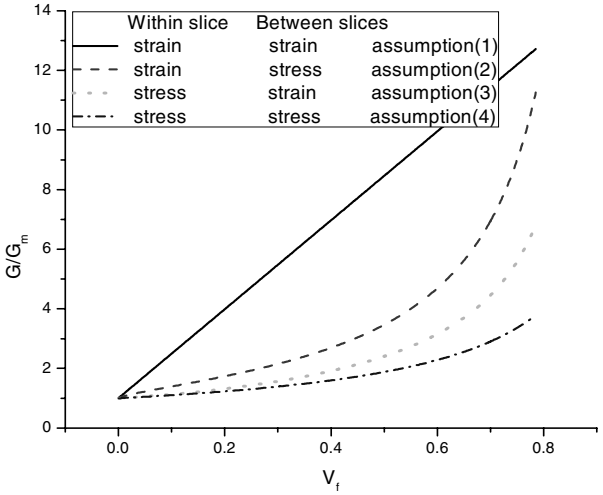

Figure 2. The variation of G/Gm with Vf.

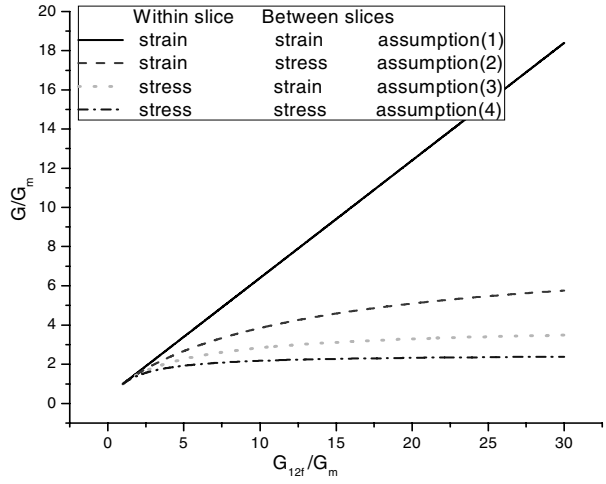

Figure 3.—The variation of G/Gm with Gf/GM

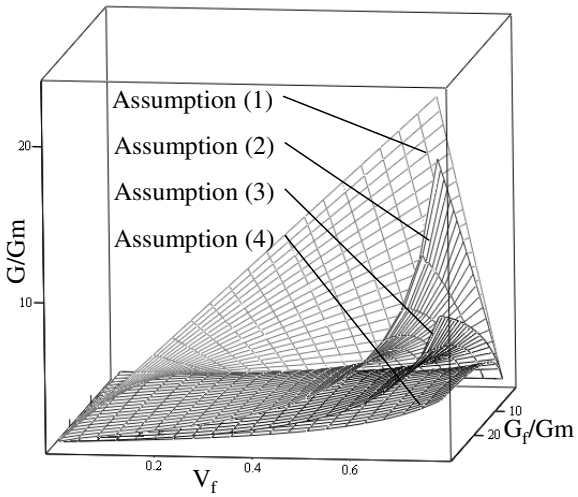

Figure 4.—The variation of G/Gm with Gf/GM and Vf.

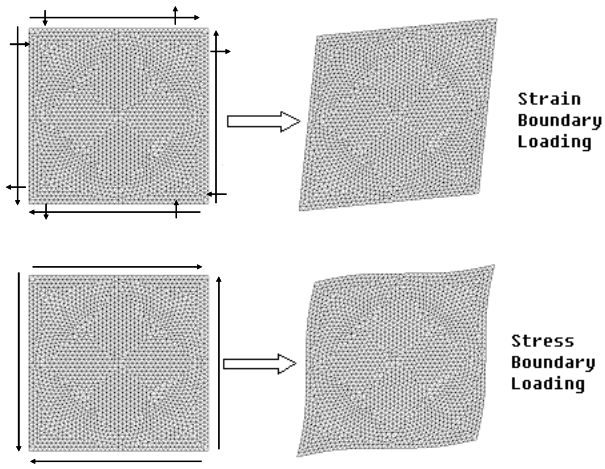

Figure 5.—Stress and strain boundary condition.

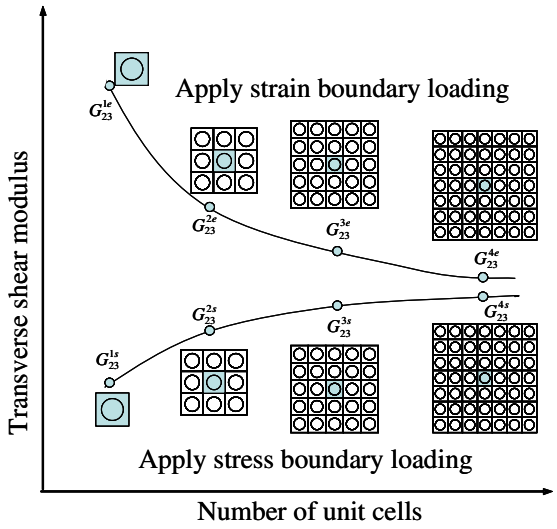

Figure 6.—Calculation of transverse shear modulus, G23.

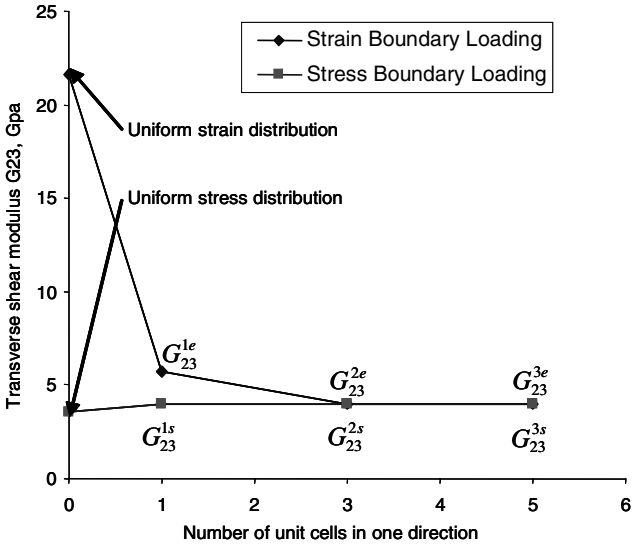

Figure 7.—Shear moduli under different boundary loadings.

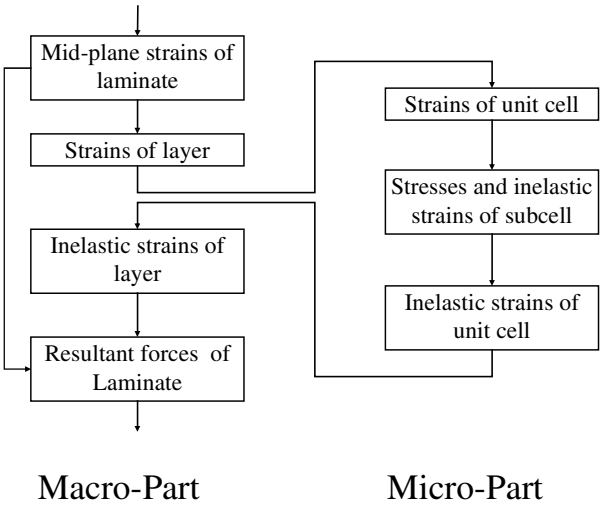

Figure 8.—Illustration of analysis procedure.

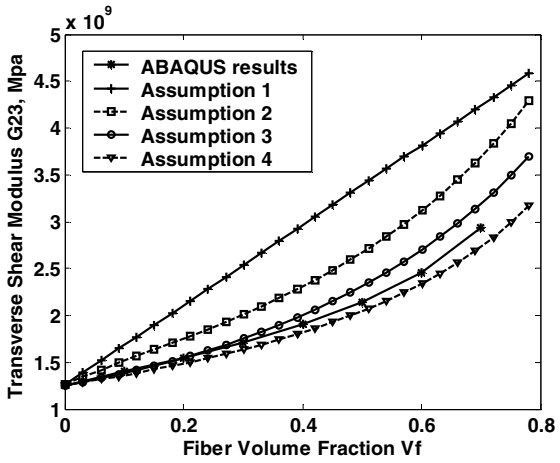

Figure 9.—Variation of G23 with Vf.

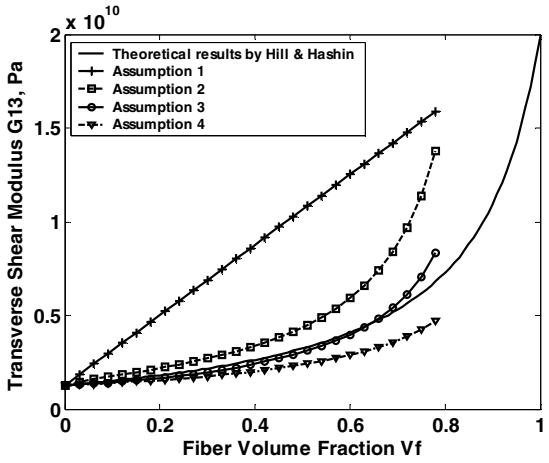

Figure 10.—Variation of G13 with Vf.

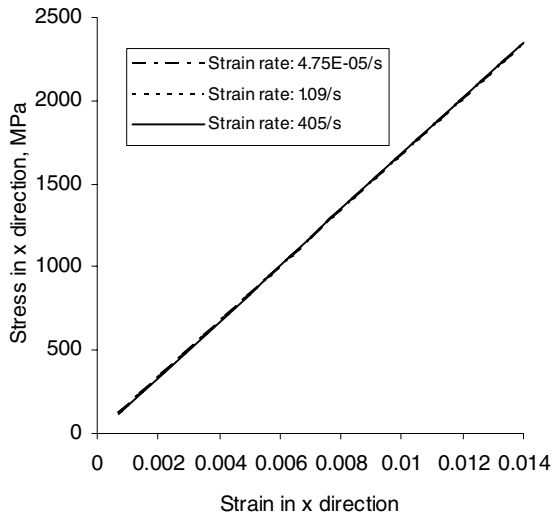

(a)

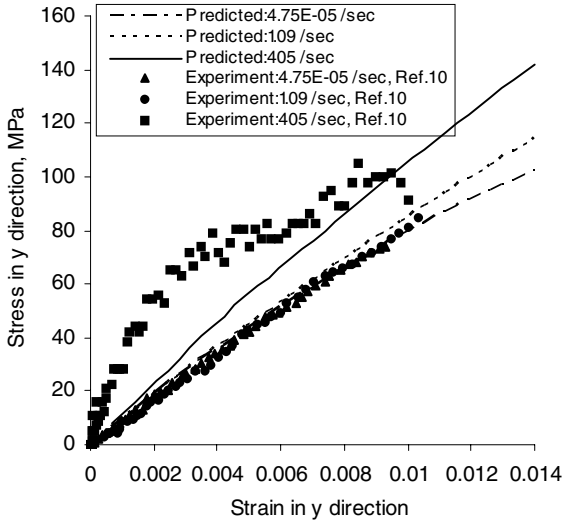

(b)

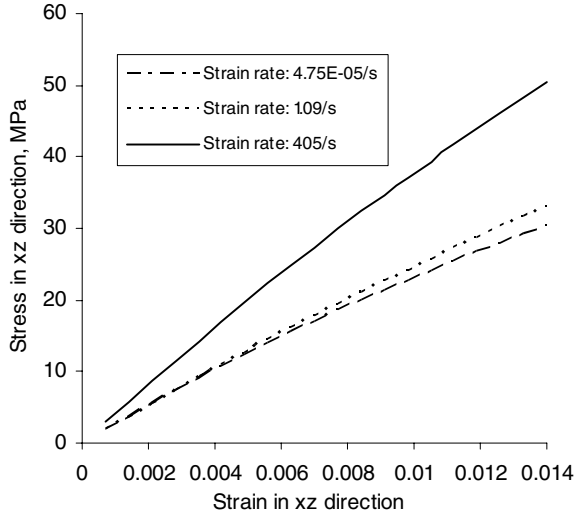

(c)

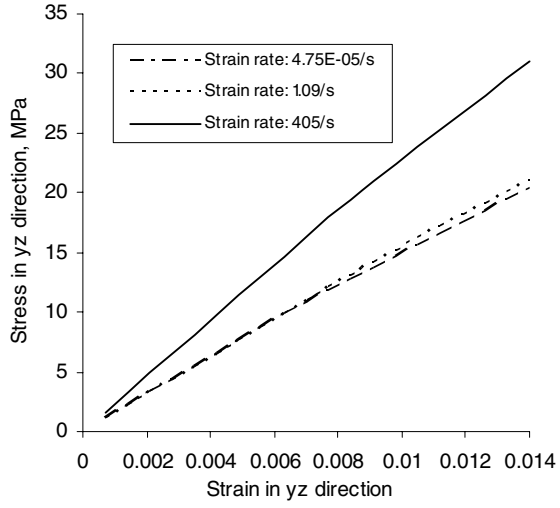

(d)

Figure 11.—Comparison of stress-strain curves of composite with stacking sequence [0°]2s at different strain rate loadings. (a) In x direction; (b) In y direction; (c) In xz direction; (d) In yz direction.

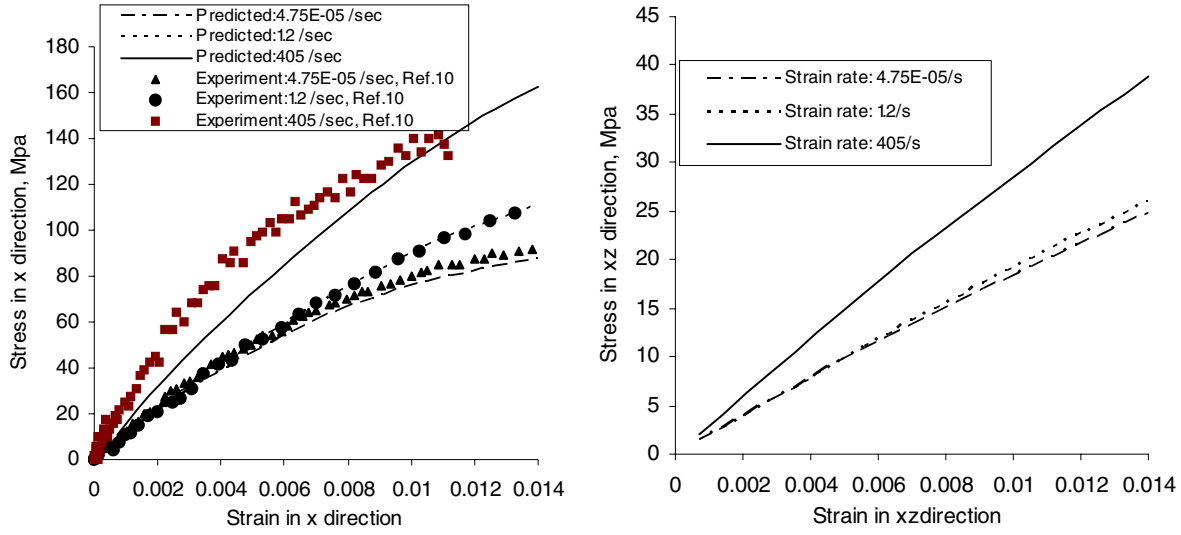

(a) (b)

Figure 12.—Comparison of stress-strain curves of composite with stacking sequence [45°]2s at different strain rate loadings. (a) In x direction; (b) In xz direction.

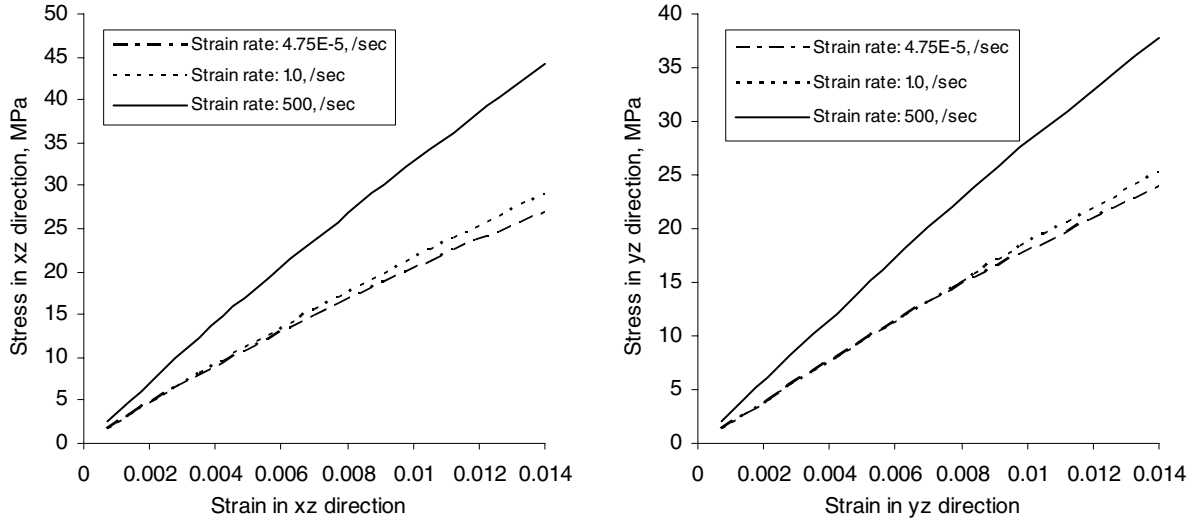

(a) (b)

Figure 13.—Comparison of stress-strain curves of composite with stacking sequence [0°/90°]s at different strain rate loadings. (a) In xz direction; (b) In yz direction.

REPORT DOCUMENTATION PAGE

Form Approved
OMB No. 0704-0188

1. AGENCY USE ONLY (*Leave blank*)	2. REPORT DATE	3. REPORT TYPE AND DATES COVERED
	December 2004	Technical Memorandum

4. TITLE AND SUBTITLE

Implementation of Improved Transverse Shear Calculations and Higher Order Laminate Theory Into Strain Rate Dependent Analyses of Polymer Matrix Composites

5. FUNDING NUMBERS

WBS–22–714–30–02

6. AUTHOR(S)

Linfa Zhu, Heung Soo Kim, Aditi Chattopadhyay, and Robert K. Goldberg

7. PERFORMING ORGANIZATION NAME(S) AND ADDRESS(ES)

National Aeronautics and Space Administration
John H. Glenn Research Center at Lewis Field
Cleveland, Ohio 44135–3191

8. PERFORMING ORGANIZATION REPORT NUMBER

E–14946

9. SPONSORING/MONITORING AGENCY NAME(S) AND ADDRESS(ES)

National Aeronautics and Space Administration
Washington, DC 20546–0001

10. SPONSORING/MONITORING AGENCY REPORT NUMBER

NASA TM—2004-213420
AIAA–2004–1638

11. SUPPLEMENTARY NOTES

Prepared for the 45th Structures, Structural Dynamics, and Materials Conference cosponsored by the AIAA, ASME, ASCE, AHS, and ASC, Palm Springs, California, April 19–22, 2004. Linfa Zhu, Heung Soo Kim, and Aditi Chattopadhyay, Arizona State University, Department of Mechanical and Aerospace Engineering, Tempe, Arizona 85287–6106; and Robert K. Goldberg, NASA Glenn Research Center. Responsible person, Robert K. Goldberg, organization code RSL, 216–433–3330.

12a. DISTRIBUTION/AVAILABILITY STATEMENT

Unclassified - Unlimited
Subject Category: 24 Distribution: Nonstandard

Available electronically at http://gltrs.grc.nasa.gov

This publication is available from the NASA Center for AeroSpace Information, 301–621–0390.

12b. DISTRIBUTION CODE

13. ABSTRACT ***(Maximum 200 words)***

A numerical procedure has been developed to investigate the nonlinear and strain rate dependent deformation response of polymer matrix composite laminated plates under high strain rate impact loadings. A recently developed strength of materials based micromechanics model, incorporating a set of nonlinear, strain rate dependent constitutive equations for the polymer matrix, is extended to account for the transverse shear effects during impact. Four different assumptions of transverse shear deformation are investigated in order to improve the developed strain rate dependent micromechanics model. The validities of these assumptions are investigated using numerical and theoretical approaches. A method to determine through the thickness strain and transverse Poisson's ratio of the composite is developed. The revised micromechanics model is then implemented into a higher order laminated plate theory which is modified to include the effects of inelastic strains. Parametric studies are conducted to investigate the mechanical response of composite plates under high strain rate loadings. Results show the transverse shear stresses cannot be neglected in the impact problem. A significant level of strain rate dependency and material nonlinearity is found in the deformation response of representative composite specimens.

14. SUBJECT TERMS

Polymer matrix composites; Strain rate; Viscoplasticity; Impact; Micromechanics

15. NUMBER OF PAGES

28

16. PRICE CODE

17. SECURITY CLASSIFICATION OF REPORT	18. SECURITY CLASSIFICATION OF THIS PAGE	19. SECURITY CLASSIFICATION OF ABSTRACT	20. LIMITATION OF ABSTRACT
Unclassified	Unclassified	Unclassified	